JOURNAL OF COMPUTATIONAL PHYSICS 36, 20–34 (1980)

Transport of Terrestrial γ Radiation in Plane Semi-Infinite Geometry

P. KIRKEGAARD AND L. LØVBORG

Risø National Laboratory, DK-4000 Roskilde, Denmark

Received February 13, 1979; revised July 9, 1979

The plane one-dimensional photon transport equation is solved for the scattered γ-radiation flux in the case of two adjacent media. One medium represents a natural ground with uniformly distributed potassium, uranium, and thorium γ-ray emitters. The other medium is air with no radioactive contaminants. The solution method is the double-P_1 approximation with equidistant lethargy mesh. By this approach, which is discussed in some detail, it is possible to calculate the complete terrestrial γ-radiation field in an economical way. Calculated ground-level γ-ray exposure rates for igneous rocks with effective atomic numbers in the range 13.1 to 15.5 are presented.

1. INTRODUCTION

Prediction of the radiation flux from the natural γ-ray emitters in the ground can be done through solution of Boltzmann's transport equation. We shall make the basic idealization of the problem geometry indicated in Fig. 1: Two semi-infinite, homogeneous media, I and II, border on each other along a plane interface a–a under which there are spatially uniform emitters with a composite line spectrum in the general case. For such a two-medium problem the double-P_l polynomial expansion method provides an efficient solution. The double-P_1 approximation (DP1) has been used by others to solve related problems: Bennett and Beck [3] compared DP1 with other polynomial expansion methods, Beck and de Planque [1] used DP1 (and P3) approximations to calculate exposure rates; and Gerstl [5, 6] solved a photon transport problem for a uniform slab in vacuum using DP1. The present model is a considerable improvement of an earlier version [10, 14] for which we have experimental confirmation [13]. The calculation procedure differs significantly from those in [3, 5, 10]. In particular the low-energy tail of the flux spectrum is calculated very efficiently. Although we developed a program system specifically for the terrestrial radiation field, we believe that the model may be useful in fallout or shielding calculations as well. The uncollided part of the radiation flux can be calculated analytically, so here we shall consider the scattered component only.

0021-9991/80/070020–15$02.00/0

2. DP1 Approximation to the Transport Equation

A brief formulation of the double-P_1 approximation for photon transport is given below in a notation similar to that used in [5]. The plane one-dimensional photon transport equation is

$$(\omega\, \partial/\partial z + \mu(z, \lambda))\, I(z, \omega, \lambda) = \int_{\lambda-2}^{\lambda} \int_{4\pi} I(z, \omega', \lambda')\, k(z, \lambda', \lambda)\, \delta(1 + \lambda' - \lambda - \boldsymbol{\Omega} \cdot \boldsymbol{\Omega}')/2\pi\, d\boldsymbol{\Omega}'\, d\lambda' + Q(z, \omega, \lambda), \qquad -\infty < z < \infty. \tag{1}$$

Here I is the differential and angular energy flux of photons, and z is the distance along the z-axis (Fig. 1). $\boldsymbol{\Omega}$ is a unit vector in the direction of photon movement,

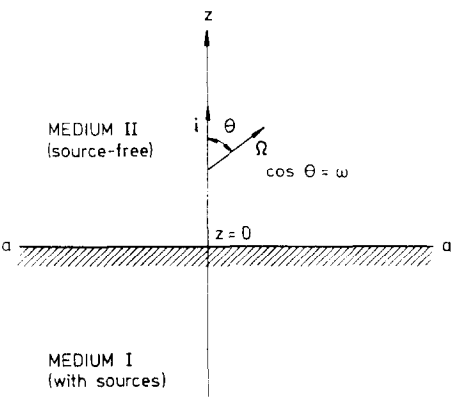

FIG. 1. Geometry for the two-medium γ-ray transport problem.

$\omega = \cos\theta = \mathbf{i} \cdot \boldsymbol{\Omega}$, where $\mathbf{i}$ is the z unit vector. λ is the wavelength in Compton units, μ is the total macroscopic cross section without coherent scattering, and Q is the differential and angular density of the energy emitted from the sources. The kernel in the scattering integral is given by the Klein–Nishina formula

$$k(z, \lambda', \lambda) = 3/8\, n_e(z)\, \sigma_0\, \lambda'/\lambda\, (\lambda/\lambda' + \lambda'/\lambda - 1 + (1 - \lambda + \lambda')^2) \tag{2}$$

for $\lambda - 2 \leqslant \lambda' \leqslant \lambda$, and 0 otherwise. λ' is the wavelength prior to scattering, and $n_e(z)$ is the electron density. σ_0 denotes the Thomson cross section in the free-electron model, but here we permit a slight variability, $\sigma_0 = \sigma_0(z, \lambda')$, with elemental composition (and consequently with z) and with λ'. It is then possible to integrate (2) up to match exactly the incoherent scattering cross section taken from a standard tabulation. The energy flux I may be split into an uncollided part U and a scattered part Ψ:

$$I(z, \omega, \lambda) = U(z, \omega, \lambda) + \Psi(z, \omega, \lambda),$$

where Ψ satisfies the transport equation

$$(\omega\,\partial/\partial z + \mu(z,\lambda))\,\Psi(z,\omega,\lambda) = \int_{\lambda-2}^{\lambda}\int_{4\pi}[\Psi(z,\omega',\lambda') + U(z,\omega',\lambda')]\,k(z,\lambda',\lambda) \cdot \delta(1+\lambda'-\lambda-\boldsymbol{\Omega}\cdot\boldsymbol{\Omega}')/2\pi\,d\boldsymbol{\Omega}'\,d\lambda', \qquad -\infty < z < \infty, \tag{3}$$

with the boundary conditions

$$\Psi(\pm\infty,\omega,\lambda) < \infty, \tag{4a}$$

$$\Psi(-0,\omega,\lambda) = \Psi(+0,\omega,\lambda). \tag{4b}$$

The basic idea of the double-P_l technique is to expand the upstreaming and the downstreaming flux in separate half-range spherical harmonics. Let $\Psi^{\pm}(z,\omega,\lambda) = \Psi(z,\omega,\lambda)\,H(\pm\omega)$, where $H(x)$ is the Heaviside function, such that $\Psi(z,\omega,\lambda) = \Psi^{+}(z,\omega,\lambda) + \Psi^{-}(z,\omega,\lambda)$ for all ω. The proper form of the expansion is

$$\Psi^{\pm}(z,\omega,\lambda) = \sum_{l=0}^{\infty}(2l+1)\,\Psi_l^{\pm}(z,\lambda)\,P_l^{\pm}(\omega) \tag{5a}$$

with the half-range moments given by

$$\Psi_l^{\pm}(z,\lambda) = \int^{\pm}\Psi(z,\omega,\lambda)\,P_l^{\pm}(\omega)\,d\omega, \tag{5b}$$

where we have used the abbreviations

$$P_l^{\pm}(\omega) \equiv P_l(2\omega \mp 1)\,H(\pm\omega), \qquad \int^{+} \equiv \int_0^1, \qquad \text{and} \qquad \int^{-} \equiv \int_{-1}^0;$$

P_l stands for the usual Legendre polynomials. If (5a) is substituted in (3), and $\delta(1+\lambda'-\lambda-\boldsymbol{\Omega}\cdot\boldsymbol{\Omega}')/2\pi$ expanded in full-range spherical harmonics in $\boldsymbol{\Omega}\cdot\boldsymbol{\Omega}'$, the result is an infinite set of interlinked integrodifferential equations satisfied by $\Psi_l^{\pm}(z,\lambda)$:

$$\tfrac{1}{2}l/(2l+1)\,\partial\Psi_{l-1}^{\pm}/\partial z \pm \tfrac{1}{2}\partial\Psi_l^{\pm}/\partial z + \tfrac{1}{2}(l+1)/(2l+1)\,\partial\Psi_{l+1}^{\pm}/\partial z + \mu(z,\lambda)\,\Psi_l^{\pm} = \tfrac{1}{2}\sum_{n=0}^{\infty}(2n+1)\,c_{nl}^{\pm}\int_{\lambda-2}^{\lambda}k(z,\lambda',\lambda)\,P_n(\gamma) \cdot \sum_{m=0}^{n}(2m+1)[(\Psi_m^{+}+U_m^{+})\,c_{nm}^{+} + (\Psi_m^{-}+U_m^{-})\,c_{nm}^{-}]\,d\lambda', \quad l = 0,1,2,\ldots. \tag{6}$$

Here we have introduced the scattering cosine γ, which for Compton scattering is equal to $1-\lambda+\lambda'$. $U_m^{\pm}$ are expansion coefficients for the two components $U^{\pm}$ of the

uncollided flux U, defined in the same way as in (5); they are supposed to be calcuculated analytically from U. $\Psi_m^{\pm}$ and $U_m^{\pm}$ are both functions of z and λ'. The numbers $c_{nm}^{\pm}$ are defined as the integrals $\int^{\pm} P_n(\omega)\, P_m^{\pm}(\omega)\, d\omega$; properties of the half-range spherical harmonics $P_l^{\pm}(\omega)$ and of $c_{nm}^{\pm}$ are listed, e.g., in [5]. From among the different ways of truncating (6) to obtain a DP1 approximation we have chosen to set $\Psi_l^{\pm} = U_l^{\pm} = 0$, $\forall l > 1$. This leaves us with a set of four equations to be solved for the four functions $\Psi_0^{\pm}(z, \lambda)$ and $\Psi_1(z, \lambda)$. We collect these flux components in a vector

$$\boldsymbol{\psi}(z, \lambda) = (\Psi_0^{+}(z, \lambda), \Psi_1^{+}(z, \lambda), \Psi_0^{-}(z, \lambda), \Psi_1^{-}(z, \lambda)). \tag{7a}$$

Similarly we define

$$\mathbf{u}(z, \lambda) = (U_0^{+}(z, \lambda), U_1^{+}(z, \lambda), U_0^{-}(z, \lambda), U_1^{-}(z, \lambda)) \tag{7b}$$

and obtain a single matrix equation:

$$\begin{aligned} \partial\boldsymbol{\psi}(z, \lambda)/\partial z &= \mu(z, \lambda)\, \mathbf{M}\boldsymbol{\psi}(z, \lambda) \\ &\quad + \int_{\lambda-2}^{\lambda} k(z, \lambda', \lambda)\, \mathbf{P}(\gamma)(\boldsymbol{\psi}(z, \lambda') + \mathbf{u}(z, \lambda'))\, d\lambda', \end{aligned} \tag{8}$$

where

$$\mathbf{M} = \begin{bmatrix} -3 & 3 & 0 & 0 \\ 1 & -3 & 0 & 0 \\ 0 & 0 & 3 & 3 \\ 0 & 0 & 1 & 3 \end{bmatrix}. \tag{9}$$

As indicated, $\mathbf{P}(\gamma)$ is a matrix whose elements depend on the scattering cosine γ; in fact we have

$$\mathbf{P}(\gamma) = \begin{bmatrix} a & b & c & d \\ e & f & g & h \\ -c & d & -a & b \\ g & -h & e & -f \end{bmatrix}, \tag{10}$$

where

$$\begin{aligned} a &= 3A - 3C, & b &= 9C - 9E, & c &= 3B + 3D, & d &= 9D - 9F, \\ e &= -A + 3C, & f &= -3C + 9E, & g &= -B - 3D, & h &= -3D + 9F, \end{aligned}$$

and where the new coefficients are the infinite series

$$\begin{aligned} A &= s(c_{n0}^{+}, c_{n0}^{+}), & B &= s(c_{n0}^{+}, c_{n0}^{-}), & C &= s(c_{n0}^{+}, c_{n1}^{+}), \\ D &= s(c_{n0}^{+}, c_{n1}^{-}), & E &= s(c_{n1}^{+}, c_{n1}^{+}), & F &= s(c_{n1}^{+}, c_{n1}^{-}), \end{aligned} \tag{11}$$

with

$$s(\alpha_n, \beta_n) \equiv \tfrac{1}{2} \sum_{n=0}^{\infty} (2n + 1)\, \alpha_n \beta_n P_n(\gamma).$$

Although stated here as infinite sums, these coefficients are expressible in analytic form in terms of γ; we shall return to this point later.

3. Computational Procedure

The numerical method for the solution of Eq. (8) is a nested procedure with the wavelength λ in the outer loop and the distance z in the inner. We shall first consider the outer integration, which starts at the shortest wavelength (highest energy in the source spectrum) and terminates when some cutoff limit is reached.

Traditional methods use an equally spaced wavelength mesh either in the total range or in different parts of it. Advantages of this method are:

(i) Values of $\gamma = 1 - \lambda + \lambda'$ are confined to an equidistant grid in $[-1, 1]$, which means that the elements of $\mathbf{P}(\gamma)$ can be precalculated from (11);

(ii) the scattering integral in (8) extends over a fixed number of steps $\Delta\lambda$, thus promoting an easy and a stable quadrature procedure; and

(iii) the eigenvalue problem is 2×2 block diagonal.

A drawback is that such a mesh leads to an excessive number of integration points at low energies so that the cost of calculation increases roughly 10 times when the energy cutoff is lowered from 100 to 10 keV. In [10] this imposed a practical limit in the cutoff of 100 keV. Others, e.g., [3], work with subintervals in which the step length $\Delta\lambda$ is constant, and, when proceeding to the next subinterval, $\Delta\lambda$ is doubled.

Our present model uses a logarithmically constant energy (or wavelength) mesh, which we believe is close to an optimal strategy. In other words, if lethargy is defined as $u = \log \lambda$, then the lethargy mesh is equidistant. An obstacle against the implementation of such a scheme is the loss of the advantages (i), (ii), and (iii) of the equidistant-λ model. We shall describe a general semianalytical wavelength integration technique which overcomes these three problems and comprises the equidistant-lethargy mesh as a particular case.

In the first place, Gerstl has shown that the infinite series in (11), $s(c_{nl}^{\pm}, c_{nm}^{\pm})$, can be expressed in closed form; in [7] he gives recursion relations and quotes these "anisotropy functions" up to $l = m = 7$. As functions of the scattering cosine γ, the anisotropy functions not only pertain to photons but also have general interest in particle scattering [6]. In the present work we shall need only the two functions

$$A(\gamma) = 1/\pi \arcsin \gamma + \tfrac{1}{2},$$
$$E(\gamma) = (3 + 4\gamma)/(3\pi) \arcsin \gamma + 4/(3\pi)\,(1 - \gamma^2)^{1/2} - 1/3\gamma - \tfrac{1}{2}.$$

(Short proofs of these formulas are given in [11].) B, C, D, and F are connected with A and E by simple relations quoted in [10]. The final expressions for the elements $(a,..., h)$ of $\mathbf{P}(\gamma)$ are shown in the Appendix, and they are simply calculated each time they are needed. Thus Gerstl's anisotropy functions are of significant importance for the successful implementation of our equidistant-u model.

In the second place we consider the quadrature process for estimation of the scattering integral in (8),

$$\mathbf{j}(z, \lambda) = \int_{\lambda-2}^{\lambda} k(z, \lambda', \lambda)\, \mathbf{P}(\gamma)\, \psi(z, \lambda')\, d\lambda' \tag{12}$$

at the current wavelength point $\lambda = \lambda_i$. A simple discrete rule, e.g., trapezoidal, in which the functions are computed at the mesh points, is unstable and will fail at low energies. This is because the complete Compton shift $(\lambda_i - \lambda' = 2)$ for small energies becomes comparable with the wavelength step $\Delta\lambda$, if Δu is constant; or even worse, it may be contained wholly within the step. It is much better to evaluate (12) using the analytical form of the Klein–Nishina kernel and the anisotropy functions. We change the integration variable from λ' to γ and suppress the argument z. Then $k(z, \lambda', \lambda) = k_0(\gamma)\, \kappa(\gamma. \lambda)$, where $k_0(\gamma) = 3/8\, n_e \sigma_0$ depends slightly on γ through σ_0, and where

$$\kappa(\gamma, \lambda) = \lambda^{-1}\gamma^3 + (\lambda^{-2} - \lambda^{-1} + 1)\gamma^2 + (-2\lambda^{-2} + \lambda^{-1})\gamma + \lambda^{-2} - \lambda^{-1} + 1.$$

The variability of k_0 is attached to $\psi(\gamma) = \psi(z, \lambda')$, assuming that the product $k_0(\gamma)\, \psi(\gamma)$ varies linearly in each interval $[\gamma_1, \gamma_2]$ between two adjacent mesh points for γ:

$$\begin{aligned} k_0(\gamma)\, \psi(\gamma) = {} & (\gamma_2 - \gamma)/(\gamma_2 - \gamma_1)\, k_0(\gamma_1)\, \psi(\gamma_1) \\ & + (\gamma - \gamma_1)/(\gamma_2 - \gamma_1)\, k_0(\gamma_2)\, \psi(\gamma_2). \end{aligned}$$

The contribution to (12) for this interval is

$$\int_{\gamma_1}^{\gamma_2} k_0(\gamma)\, \kappa(\gamma, \lambda)\, \mathbf{P}(\gamma)\, \psi(\gamma)\, d\gamma = \mathbf{W}_1 \psi(\gamma_1) + \mathbf{W}_2 \psi(\gamma_2). \tag{13}$$

If the indefinite matrix integrals $\mathbf{F}(\gamma) = \int \kappa(\gamma, \lambda)\, \mathbf{P}(\gamma)\, d\lambda$ and $\mathbf{G}(\gamma) = \int \gamma\kappa(\gamma, \lambda)\, \mathbf{P}(\gamma)\, d\gamma$ are introduced, the "weight matrices" in (13) can be written as

$$\mathbf{W}_1 = k_0(\gamma_1)/(\gamma_2 - \gamma_1)[\gamma_2(\mathbf{F}(\gamma_2) - \mathbf{F}(\gamma_1)) - (\mathbf{G}(\gamma_2) - \mathbf{G}(\gamma_1))], \tag{14a}$$

$$\mathbf{W}_2 = k_0(\gamma_2)/(\gamma_2 - \gamma_1)[-\gamma_1(\mathbf{F}(\gamma_2) - \mathbf{F}(\gamma_1)) + (\mathbf{G}(\gamma_2) - \mathbf{G}(\gamma_1))]. \tag{14b}$$

(If the interval $[\gamma_1, \gamma_2]$ encompasses the value $\gamma = \gamma_0$ corresponding to the lower limit in the integral (12), $\mathbf{F}(\gamma_1)$ and $\mathbf{G}(\gamma_1)$ in (14) should be replaced by $\mathbf{F}(\gamma_0)$ and $\mathbf{G}(\gamma_0)$).

After (12) is computed, Eq. (8) reduces to a vector equation in z for the flux at $\lambda = \lambda_i$ (suppressed in the notation below):

$$d\boldsymbol{\psi}(z)/dz = \mathbf{B}\boldsymbol{\psi}(z) + \boldsymbol{\phi}(z). \tag{15}$$

Solution of (15) makes up the inner loop of the procedure. The term $\boldsymbol{\phi}(z)$ depends on the sources for the problem and is composed of real sources and a scatter-in contribution from shorter wavelengths. Up to now, we have not specified the source term $Q(z, \omega, \lambda)$ in (1). In the following we shall assume that

$$Q(z, \omega, \lambda) = EH(-z) \sum_p q_p/4\pi\, \delta(E - E_p). \tag{16}$$

Equation (16) states that the source has a discrete line spectrum ($E = 1/\lambda$ = energy, E_p = energy of line no. p) and is confined to medium I ($z < 0$). Further, the interaction cross section $\mu(z) = \mu(z, \lambda_i)$ is assumed to be a piecewise constant function of z, $\mu(z) = \mu_{\mathrm{I}}$ for $z < 0$ and $\mu(z) = \mu_{\mathrm{II}}$ for $z > 0$. On these assumptions the uncollided flux $U(z, \omega, \lambda)$ and its half-range moments $U^{\pm}(z, \lambda)$, and hence also $\boldsymbol{\phi}(z)$, can be calculated analytically. The results, which involve exponential integrals, are given in [10]. The matrix of the differential equations (15) can be written as $\mathbf{B} = \mu(z)\mathbf{M} + \mathbf{R}(z)$, where both μ and $\mathbf{R}$ are constant in each medium. $\mathbf{R}$ can be interpreted as a perturbation matrix originating from the scattering integral (12). Contributions to $\mathbf{R}$ come exclusively from the wavelength interval $[\lambda_{i-1}, \lambda_i]$ and are normally small. If pointwise quadrature had been applied to (12) instead of an analytical technique, $\mathbf{R}$ would have been proportional to $\mathbf{M}$, thus preserving the 2×2 block diagonality for $\mathbf{B}$, and (15) could be solved by simple decoupling as in [10]. Our third problem is that we get "fill-in" into the bidiagonal blocks of $\mathbf{R}$ as a consequence of the analytical operations on (12). This is a minor complication, because it is still true that the eigenproblem for $\mathbf{B}$ only involves solution of a quadratic equation. To see this, we note that $\mathbf{B}$ is of the general class (10) ($(a,..., h)$ are in this context arbitrary numbers) because $\mathbf{B}$ is the result of scalar operations (including integrations) on $\mathbf{M}$ and $\mathbf{P}(\gamma)$. The characteristic polynomial for such a matrix is

$$\begin{aligned} p(\sigma) = {} & \sigma^4 + (c^2 - a^2 + h^2 - f^2 - 2be - 2dg)\,\sigma^2 + (af + dg)^2 \\ & + (be + ch)^2 - (bg + ah)^2 - (cf + de)^2 - 2(ae - cg)(bf - dh). \end{aligned}$$

In the limiting case $\mathbf{R} = \mathbf{0}$ there are two pairs of real roots ($\sigma = \pm(3 \pm 3^{1/2})\,\mu(z)$), and for $\| \mathbf{R} \|$ not too large this will still be the case. Hence the eigenvalues $\{\sigma_1, \sigma_2, \sigma_3, \sigma_4\}$ can be ranked such that $\sigma_1 < \sigma_2 < 0 < \sigma_3 < \sigma_4$ with $\sigma_1 = -\sigma_4$ and $\sigma_2 = -\sigma_3$. Diagonalization of (15) results in the transformed equation

$$d\boldsymbol{\chi}(z)/dz = \boldsymbol{\Sigma}\boldsymbol{\chi}(z) + \mathbf{Y}^{-1}\boldsymbol{\phi}(z), \tag{17}$$

where $\boldsymbol{\Sigma} = \mathrm{diag}\{\sigma_1, \sigma_2, \sigma_3, \sigma_4\}$, and the transformation matrix $\mathbf{Y}$ contains the

eigenvectors as columns. There is an equation (17) for each medium ($p = 1, 2$), and each represents four ($m = 1, 2, 3, 4$) independent scalar equations:

$$dX_{mp}(z)/dz = \sigma_{mp} X_{mp}(z) + h_{mp}(z). \tag{18}$$

Also in the z-integration analytical tools are used to some extent. To simplify notation, we shall drop the indices m and p. Then (18) has the complete solution

$$X(z) = \exp(\sigma z) \left\{ \int \exp(-\sigma z)\, h(z)\, dz + C \right\}. \tag{19}$$

The analytical form of $X(z)$ is not a simple one because $h(z)$ is a complicated function: It contains exponential integrals with rapidly increasing complexity as the wavelength integration proceeds. Therefore, an approximate method is applied. The source term is written as a stationary term plus a decaying exponential multiplied by a polynomial of degree k:

$$h(z) \approx h_\infty + \exp(\alpha z) \sum_{j=0}^{k} h_j z^j, \tag{20}$$

where $\alpha > 0$ if $p = 1$ and $\alpha < 0$ if $p = 2$. h_∞ can be found analytically, while the other parameters must be determined in the least-squares sense: Operating with a fixed set $\{z_i\}$ of points in the medium we first calculate $h(z_i)$ from the solution in z_i at shorter wavelengths, and thereafter we execute the semilinear least-squares procedure described by Kirkegaard and Eldrup [9]. This procedure iterates on the nonlinear parameter α only and is therefore fast. (However, in the low-energy range, α could safely be fixed to a precalculated value, thereby increasing both speed and stability.) We have selected the point set $\{z_i\}$ in such a way that the distances from the interface $z = 0$ increased logarithmically; further details of the fitting procedure are given in [10]. Merging (19) and (20) leads to the following solution for the transformed flux:

$$X(z) = X_\infty + C \exp(\sigma z) + \exp(\alpha z) \sum_{j=0}^{k} \kappa_j z^j, \tag{21}$$

where

$$\begin{aligned} X_\infty &= -h_\infty/\sigma, \\ \kappa_k &= h_k/(\alpha - \sigma), \\ \kappa_j &= (h_j - (j+1)\,\kappa_{j+1})/(\alpha - \sigma), \qquad j = k-1, \ldots, 0. \end{aligned}$$

Precautions are taken to keep $|\alpha - \sigma|$ greater than some small number ϵ. The integration constants $C = C_{mp}$ are determined from the boundary conditions (4); from (4a) and the signs of the eigenvalues we infer that $C_{11} = C_{21} = C_{32} = C_{42} = 0$. The other condition is a little more complicated to express. Since the transformation matrix $\mathbf{Y} = \mathbf{Y}_p$ depends on the medium, we must equalize the untransformed fluxes

$\psi(\pm 0)$ and not χ. The result is that the remaining four constants, collected in the vector $\mathbf{c} = (C_{12}, C_{22}, C_{31}, C_{41})$, satisfy the 4th-order system

$$\mathbf{Y}^*\mathbf{c} = \mathbf{Y}_2\boldsymbol{\chi}_{2.}^* - \mathbf{Y}_1\boldsymbol{\chi}_{1.}^*$$

where $\boldsymbol{\chi}_p^*$ is the value that the transformed flux vector in medium p would assume for $z = 0$, if $C = C_{mp}$ were zero in (21); the coefficient matrix $\mathbf{Y}^*$ has its two first colums equal to the two first in $-\mathbf{Y}_2$, and the two last columns equal to the two last in $\mathbf{Y}_1$. We might, finally, be interested in handling the particular case in which medium II is vacuum. Condition (4b) is then replaced by the requirement that $\Psi(0, \omega, \lambda) = 0$ for $\omega < 0$, i.e., the "downstreaming" moments Ψ_0^- and Ψ_1^- are set to zero for $z = 0$.

It may be asked how the accuracy and the computing efficiency of the model described compare with what is obtained by conventional integration schemes for the photon transport equation. To a first approximation we can study this problem independently for the three variables ω, z, and λ.

Errors in the angular flux distributions are mainly due to truncation errors in the DP1 approximation itself. Concerning the z-integration, we have tested our least-squares procedure using nine points in each medium and a fitting polynomial of the second degree in (20). Dose rates in air at various heights were computed, and from Table I it is seen that the results agree well with similar data obtained by Beck and de Planque [1], who used a purely numerical integration method.

TABLE I

Absorbed Dose Rates (1 MeV/g/sec = 66.37 μR/hr) Calculated for Terrestrial Potassium-40 γ Radiation (cf. [1])

	Dose rate (MeV/g/sec)	
z (m)	This work	Beck and de Planque [1]
0	0.438	0.436
30	0.317	0.316
100	0.185	0.185
300	0.0506	0.0499

It remains to consider the effect of our treatment of the wavelength λ, which is the crucial point in the model. Of particular interest is to compare the equidistant-lethargy scheme with the equidistant-wavelength scheme. For this purpose we coded both procedures identically in all respects other than the λ-integration.

We computed the spectral distribution of potassium γ radiation at the interface between air and soil down to 40 keV. The constant-$\Delta\lambda$ model was run with $\Delta\lambda = 1/7$ (case I) and the constant-Δu model with $\Delta u = 0.06$ (case II), leading to 89 and 61 mesh points, respectively. As the cost per mesh point was almost 50% greater in case II, the two computations represented roughly the same total work. The low-

energy part of the computed spectra is shown in Fig. 2 together with a reference calculation with an adjoint Monte Carlo code based on a work of Kalos [8] (SD $\approx$ 1.7% in each spectral channel).

The results from II lie significantly closer to the Monte Carlo spectrum than those from I. The difference between the two DP1 spectra is about 4% over most of the range. The models are consistent in the sense that the spectra would coincide if both meshes were made arbitrarily fine. We also computed the energy flux integrals from 40 keV to 1.461 MeV of spectra I and II and compared them with the integral of the Monte Carlo spectrum which was normalized to 1.000 (with SD $\approx$ 0.002). The results were 1.030 in case I and 0.995 in case II.

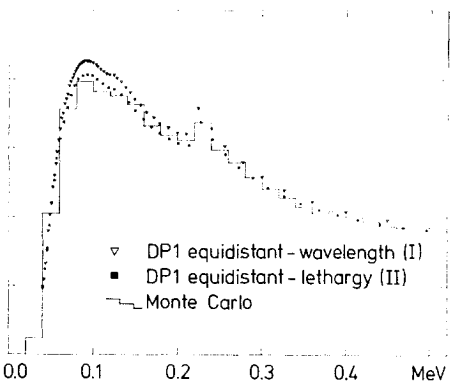

FIG. 2. Spectral distribution below 0.5 MeV of scattered potassium-40 γ radiation at the interface (energy flux).

A closer investigation reveals that the poorer accuracy in case I stems from the discretization error committed in the evaluation of the scattering integral at high energies, where the Klein–Nishina kernel $k(z, \lambda', \lambda)$ is a strongly convex function of λ' owing to the marked anisotropy. The error propagates down to the low energies and gives a bias to the entire spectrum. Such a discretization error does not exist in case II where the scattering integral is evaluated semianalytically. Admittedly another error arises here, because $k_0(\gamma)\ \psi(z, \lambda')$ is linearized between the mesh points. This error is, however, of the second order when $k_0(\gamma)\ \psi(z, \lambda')$ varies slowly compared to $k(z, \lambda', \lambda)$, as it actually does in most of the range. Exceptions are the steps which include a discontinuity point for $\psi(z, \lambda')$ or $\partial/\partial\lambda'\psi(z, \lambda')$.

The stability of our method with respect to the length of the step Δu is in practice unlimited. In the example of Fig. 2 the eigenvalues were all real for any value of Δu. Even with $\Delta u = 0.24$ the correct spectrum was fairly well reproduced and the normalized flux integral was found to be 0.989. However, computations on general terrestrial radiation problems with many source lines require a much smaller Δu.

It is important to notice that the constant-Δu procedure is only one out of many possible integration schemes based on the semianalytical technique. One could in principle use any nonequidistant set of wavelength points and, for instance, take

very small steps where the flux is known to have jumps. These possibilities were not exploited in this work in which the equidistant-lethargy scheme proved to be a reasonable compromise between simplicity and overall efficiency.

4. Results

A FORTRAN program GAMP1 has been written based on the method described. The output from this program is the parameters in (21) for the transformed flux components together with the transformation matrix **Y**. With these data given for both media and for all the mesh points of λ it is easy to evaluate the expansion coefficients $\Psi_0^{\pm}(z, \lambda)$ and $\Psi_1^{\pm}(z, \lambda)$ for all z and λ. Subsequent use of the truncated form of (5a),

$$\begin{aligned} \Psi(z, \omega, \lambda) &\approx \Psi_0^{+}(z, \lambda) + 3\Psi_1^{+}(z, \lambda)(2\omega - 1), \qquad 0 < \omega < 1, \\ &\approx \Psi_0^{-}(z, \lambda) + 3\Psi_1^{-}(z, \lambda)(2\omega + 1), \qquad -1 < \omega < 0, \end{aligned}$$

will permit a reconstruction of the complete radiation field. Another program, GFX, calculates the integral field quantities flux and dose for arbitrary z, using the GAMP1 output. The γ-ray sources are supposed to be potassium-40 or the emitters in the natural decay series of uranium and thorium. Auxiliary programs have been written for handling of input data, and the complete program system is described in [11]. It is in operation at the Burroughs 6700 installation at Risø and is available from the NEA Data Bank.

Figures 3–6 illustrate various features of the scattered part of a terrestrial γ-radiation field. From plots like these it has been demonstrated that such a field is described in sufficient detail by using a lethargy step of $\Delta u = 0.03$ and a fitting polynomial degree of $k = 2$ in (20), and also that a cutoff energy of 20 keV is reasonable. The spatial variations of the four DP1 moments are exemplified in Fig. 3. Figure 4 shows

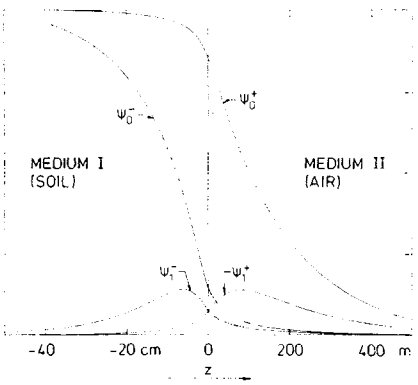

FIG. 3. Spatial variation of the DP1 moments for scattered uranium γ radiation at 700 keV.

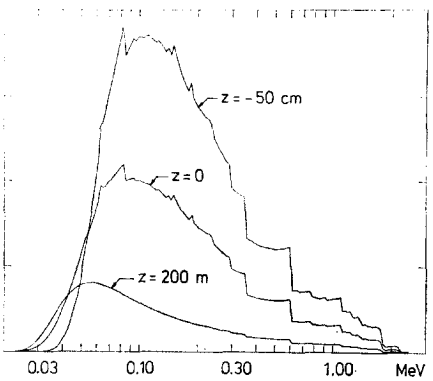

FIG. 4. Spectral distributions of scattered uranium γ radiation (energy flux).

the spectral distribution of scattered uranium γ-radiation in the soil ($z = -50$ cm), at ground level ($z = 0$), and high up in the air ($z = 200$ m). It is seen that this variation in z is accompanied by a loss of radiation intensity and spectral detail, and there is a spectral shift towards lower energies. These phenomena are further illustrated in Fig. 5, and Fig. 6 demonstrates the omnidirectional nature of a scattered flux of low-energy γ rays.

Table II shows the exposure rates at $z = 1$ m per unit concentration of potassium, uranium, and thorium in typical soil (assuming radioactive equilibrium in the uranium–thorium decay series). Agreement is found with the results of Beck and co-workers [2].

The predominant γ-ray interaction mode in soil or rock is incoherent scattering. However, a significant concentration in the ground material of a heavy element such as iron increases the proportion of photoelectric absorption at low energies. The absorption properties of a mixture of elements are conveniently expressed in terms

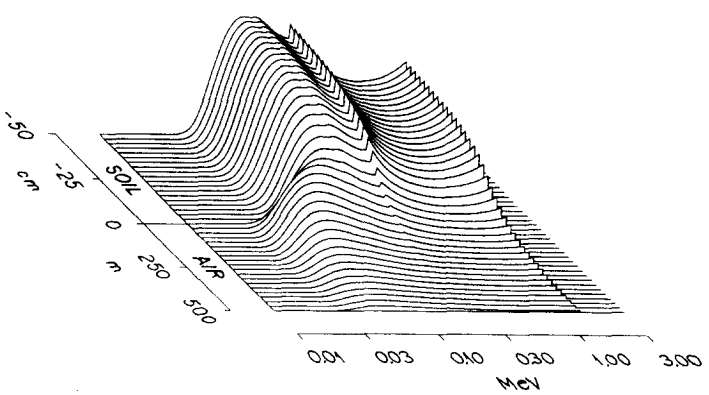

FIG. 5. Spectral and spatial distribution of scattered potassium-40 γ radiation (energy flux).

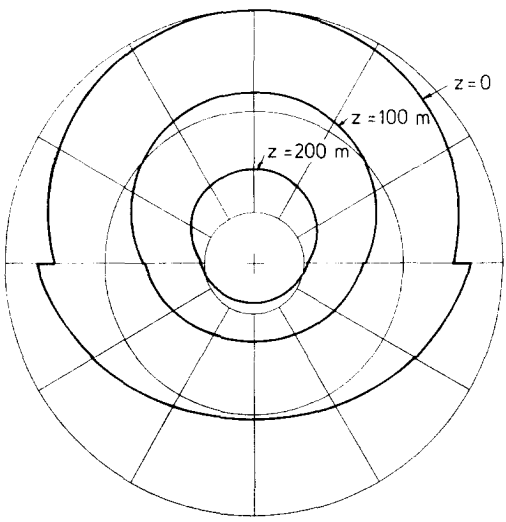

FIG. 6. Angular distributions per unit solid angle of scattered uranium γ radiation at 100 keV reconstructed from the DP1 moments. Top orientation corresponds to $\theta = 0°$ ($\omega = 1$).

TABLE II

Calculated γ-Ray Exposure Rates from Potassium, Uranium, and Thorium 1 m over Typical Soil

	Exposure rate (μR/hr)	
	This work	Beck *et al.* [2]
1 % K	1.505	1.49
1 ppm U	0.619	0.62
1 ppm Th	0.305	0.31

TABLE III

γ-Ray Exposure Rates at 1 m from Potassium, Uranium, and Thorium for Four Types of Igneous Rocks

Rock type	Iron content (%)	Z_{eff} [12]	Exposure rate (μR/hr)		
			1 % K	1 ppm U	1 ppm Th
Granite	2.5	13.1	1.519	0.622	0.306
Syenite	4.4	13.9	1.516	0.618	0.304
Gabbro	6.8	14.8	1.511	0.613	0.302
Plateau basalt	10.1	15.5	1.508	0.610	0.300

of an effective atomic number, Z_{eff} [12]. In Table III four types of igneous rock of the compositions given in [4] are considered. It appears that the exposure rates produced by unit radioelement concentrations show only small, though significant, decreases when Z_{eff} increases from 13.1 to 15.5.

5. Concluding Remarks

We have presented an efficient method of solving the double-P_1 equations for photon transport in plane semi-infinite geometry. Use of an equidistant lethargy mesh with a piecewise analytical treatment of the scattering integral has been combined with a semilinear least-squares technique for the space coordinate to produce a fast and numerically stable procedure. Application of Gerstl's analytic anisotropy functions instead of truncated series ensures the exact angular representation of the very anisotropic Klein–Nishina kernel. The program system GAMP1/GFX has been applied for various assessments about flux and exposure for terrestrial γ-radiation fields. Within the same computational framework it is possible to consider other source geometries. For example, both media could be active and a spatial variation could be allowed. By such straightforward extensions, fallout or shielding problems could also be studied.

Appendix

Matrix elements of $\mathbf{P}(\gamma)$:

$$
\begin{aligned}
a &= 6/\pi \arcsin\gamma + 3/2 - 3/2\,\gamma,\\
b &= -(18+12\gamma)/\pi \arcsin\gamma - 12/\pi\,(1-\gamma^2)^{1/2} + 9/2 + 15/2\,\gamma,\\
c &= -6/\pi \arcsin\gamma + 3/2 + 3/2\,\gamma,\\
d &= -(18-12\gamma)/\pi \arcsin\gamma + 12/\pi\,(1-\gamma^2)^{1/2} - 9/2 + 15/2\,\gamma,\\
e &= -4/\pi \arcsin\gamma - 1/2 + 3/2\,\gamma,\\
f &= (12+12\gamma)/\pi \arcsin\gamma + 12/\pi\,(1-\gamma^2)^{1/2} - 9/2 - 9/2\,\gamma,\\
g &= 4/\pi \arcsin\gamma - 1/2 - 3/2\,\gamma,\\
h &= (12-12\gamma)/\pi \arcsin\gamma - 12/\pi\,(1-\gamma^2)^{1/2} + 9/2 - 9/2\,\gamma.
\end{aligned}
$$

Formulas for $\int x^n \arcsin x\,dx = S_n(x)\arcsin x + T_n(x)(1-x^2)^{1/2}$

n	$S_n(x)$	$T_n(x)$
0	x	1
1	$-1/4 + 1/2\,x^2$	$1/4\,x$
2	$1/3\,x^3$	$2/9 + 1/9\,x^2$
3	$-3/32 + 1/4\,x^4$	$3/32\,x + 1/16\,x^3$
4	$1/5\,x^5$	$8/75 + 4/75\,x^2 + 1/25\,x^4$
5	$-5/96 + 1/6\,x^6$	$5/96\,x + 5/144\,x^3 + 1/36\,x^5$

Formulas for $\int x^n(1 - x^2)^{1/2}\,dx = U_n \arcsin x + V_n(x)(1 - x^2)^{1/2}$

n	U_n	$V_n(x)$
0	1/2	$1/2\,x$
1	0	$-1/3 + 1/3\,x^2$
2	1/8	$-1/8\,x + 1/4\,x^3$
3	0	$-2/15 - 1/15\,x^2 + 1/5\,x^4$
4	1/16	$-1/16\,x - 1/24\,x^3 + 1/6\,x^5$

REFERENCES

1. H. L. BECK AND G. DE PLANQUE, HASL-195, 1968.
2. H. L. BECK, J. DE CAMPO, AND C. GOGOLAK, HASL-258, 1972.
3. B. G. BENNETT AND H. L. BECK, HASL-185, 1967.
4. S. P. CLARK, JR., *in* "Handbook of Physical Constants" (S. P. Clark, Jr., Ed.), p. 1, Geol. Soc. Amer., New York, 1966.
5. S. A. W. GERSTL, *Nukleonik* **8** (1966), 101.
6. S. A. W. GERSTL, *Nukleonik* **10** (1967), 227.
7. S. A. W. GERSTL, *J. Reine Angew. Math.* **236** (1969), 131.
8. M. H. KALOS, *Nucl. Sci. Eng.* **33** (1968), 284.
9. P. KIRKEGAARD AND M. ELDRUP, *Comput. Phys. Comm.* **3** (1972), 240.
10. P. KIRKEGAARD AND L. LØVBORG, Risø Report No. 303, 1974.
11. P. KIRKEGAARD AND L. LØVBORG, Risø Report No. 392, 1979.
12. R. M. KOGAN, I. M. NAZAROV, AND SH. D. FRIDMAN, "Gamma Spectrometry of Natural Environments and Formations," p. 46, Israel Program for Scientific Translations, No. 5778, Jerusalem, 1971.
13. L. LØVBORG AND P. KIRKEGAARD, *Nucl. Inst. Meth.* **121** (1974), 239.
14. L. LØVBORG AND P. KIRKEGAARD, Risø Report No. 317, 1975.